

The Effect of Heat Treatment on the Corrosion Resistance, Mechanical Properties and Wear Resistance of Cr–C Coatings and Cr–C/Al₂O₃ Composite Coatings Electrodeposited on Low Carbon Steel

Hung-Hua Sheu^{1,*}, Ting-Yi Hong¹, Tzu-Te Lin², Ming-Der Ger^{1,*}

¹ Department of Chemical and Materials Engineering, Chung Cheng Institute of Technology, National Defense University, Taoyuan City, Taiwan

² Department of Power Vehicle and Systems Engineering, Chung Cheng Institute of Technology, National Defense University, Taoyuan City, Taiwan

*E-mail: shhccit@gmail.com, mingderger@gmail.com

Received: 5 June 2018 / Accepted: 30 July 2018 / Published: 1 September 2018

In order to enhance the corrosion resistance, mechanical properties and wear resistance of Cr–C thin films, Cr–C/Al₂O₃ composite coating is electrodeposited from the Cr(III) plating bath containing Al₂O₃ particles in this study. The Cr–C/Al₂O₃ composite coating has the best corrosion resistance which i_{corr} is approximately at 2.84×10^{-7} A/dm², but the corrosion resistance will reduce with an increase of heating temperature due to the formation of cracks within Cr–C/Al₂O₃ composite coatings. The effect of heat treatment on the mechanical properties and tribological behavior of Cr–C coating and Cr–C/Al₂O₃ composite coating is examined. The experimental results show that the hardness of Cr–C coating and Cr–C/Al₂O₃ composite coating increased with a heat treatment process due to the precipitation of chromium carbide and chromium oxide. The incorporation of Al₂O₃ particles into the Cr–C matrix can significantly enhance the micro-hardness and reduce the wear rate of Cr–C/Al₂O₃ composite coating as compared to that of Cr–C coating. The highest micro-hardness of Cr–C/Al₂O₃ composite coatings (22.85 GPa) is achieved after the coatings heated at 600 °C. The co-deposition of Al₂O₃ particles within the Cr–C deposits will significantly improve the wear resistance of coatings and reduces the wear weight loss. The lowest specific wear rate (8.8×10^{-7} mm³/Nm) was obtained for the Cr–C/Al₂O₃ composite coatings heat treated at 200 °C.

Keywords: Cr–C/Al₂O₃ composite coating, wear rate, Cr(III) bath, heat treatment

1. INTRODUCTION

Cr–C plating from a Cr (III) electrolyte has been considered as a promising replacement for carcinogenic and toxic Cr (VI) electroplating [1-7]. However, the maximum thickness generally is less

than 10 μm [8] and cracks are frequently observed [9] for the Cr coatings electroplated from the trivalent chromium baths, which are detrimental to their wear and corrosion properties. A metal matrix composite is a good way to gain a greater wear and corrosion properties.

Ceramic particles-reinforced composite coatings have been widely developed due to their high hardness, good wear and corrosion resistance compared to pure metal or alloy coatings. Electroplating is one of the suitable methods for producing the composite coatings by co-deposition of inert particles into a metal matrix. These improved properties mainly depend on the content and nature of particles in the coatings. These inert particles including SiC, Al_2O_3 , WC, TiO_2 , Si_3N_4 , and diamond [10-16] are frequently co-deposited into metal matrices to form composite coatings. Among these particles, alumina (Al_2O_3) has many superior properties, such as low price, good chemical stability, high hardness, and wear resistance at high-temperature [17]. Therefore, as a second phase to strength composite materials, Al_2O_3 is one of the economic and powerful materials. It has been shown that modification of mechanical and electrochemical properties, including increased resistance to wear, increased corrosion resistance, and increased hardness could be achieved by incorporation of hard Al_2O_3 particles in chromium coatings [18-20].

On the other hand, it is well known that heat treatment will cause changes in microstructures of metals such as phase change, grain size, residual stress and crack, leading to the enhancement of hardness of the coatings [21-23]. Annealing at elevated temperatures has also been utilized to improve the mechanical properties of the trivalent chromium coatings. The literatures had found that with an annealing of the trivalent chromium coatings, the hardness of Cr-C coating increases due to the crystallization of chromium and precipitation of hard chromium carbides phases [2, 24]. In our previous study [25], heat treatment was utilized to improve hardness of the Cr-C- Al_2O_3 composite coating. The hardness increases with heat treatment temperature. The highest hardness (HV 1520) was found for Cr-C- Al_2O_3 composite coating annealed at 600 °C due to the precipitation of Cr_{23}C_6 and Cr_2O_3 during the treatment, whereas heat treatment at 600 °C had an inverse effect on the corrosion resistance. The possible explanation was that the precipitation of chromium carbides would increase the residual stress caused by a serious lattice distortion and form great amount of cracks within Cr-C coatings, leading to the corrosion resistance decreased after annealing at 600 °C. However, the effect of heat treatment on anti-wear behavior of trivalent Cr-C/ Al_2O_3 coatings is seldom studied. Therefore, in this work, the hardness values and wear resistance of as-plated, annealed Cr-C alloy deposits and annealed Cr-C/ Al_2O_3 composite deposits are discussed.

2. EXPERIMENTAL

The trivalent chromium coatings and chromium carbide alumina composite coatings were deposited on low carbon steel (0.2 wt% carbon) substrate having a size of 50 × 65 × 3 mm by direct current plating. The surface of substrates were ground with #2000 silicon sandpaper, degreased with acetone for 2 min, activated by 3% NaOH solution for 1 min, pickled in a hydrochloric acid solution (HCl (35%): water = 1:1) for 5 min prior to electroplating process. The trivalent chromium carbon deposits were electroplated in an electrolyte containing 0.3 M $\text{CrCl}_3 \cdot 6\text{H}_2\text{O}$ as the main metal salt, 3 M

ammonium formate as complexing agent, 0.02 M KBr, 0.6 M KCl and 0.5 M B(OH)₃. The Cr–C–Al₂O₃ composite coatings were prepared by adding 15 g/L Al₂O₃ particles with an average diameter of 0.3 μm into the plating bath. Magnetic stirring and subsequently by ultrasonic agitation for 40 min just prior to electroplating were utilized to make the dispersion of Al₂O₃ particles become uniformly. The electroplating was carried out for 1 h with the conditions of pH 4.5, temperature of 25 °C, stirring rate of 300 rpm, and current density of 20 A/dm². The as-deposited Cr–C alloy coatings and Cr–C–Al₂O₃ composite coatings were heat treated in an oven filled with nitrogen atmosphere at temperatures of 200, 400 and 600 °C, respectively, for 1 h.

The surface and cross-section morphologies of Cr–C and Cr–C–Al₂O₃ deposited specimens were examined with a field emission scanning electron microscopy (FESEM, HITACHI S-3000 N, operating at 15 kV). The crystalline structure and constituent phase of the coatings were examined by a X-ray diffraction (XRD, BRUKER D2 PHASE) with Cu K_α radiation ($\lambda = 0.15405$ nm) over a scanning range from 10° to 100°. A differential scanning calorimeter (DSC, NETZSCH DSC 404F3) was used to detect the thermal events with a heating rate of 20 °C/min from room temperature up to 700 °C.

The potentiodynamic polarization tests were carried out in a standard three-electrode cell system using an Autolab-PGSTAT30 potentiostat/galvanostat controlled by a GPES (General Purpose Electrochemical system) software and stabilized at open circuit potential (OCP) before electrochemical test. A platinum sheet and Ag/AgCl electrode were used as the counter and reference electrodes, the linear polarization curves of Cr–C and Cr–C/Al₂O₃ composite coatings were measured after 20 min immersion of specimens in a 3.5% NaCl aqueous solution at room temperature in the potential range between -0.3 V and 0.5 V with a scanning rate of 0.5 mV s⁻¹.

A Nano-Indenter XP system (NIS) made by MTS Co. Ltd. was used to measure the hardness of the films. All samples were indented with an applied load of 2500 μN. For each sample, the hardness considered is an average value of five measurements conducted at various locations. The average hardness was given directly by the NIS system. In order to ensure the absence of thermal drift, a 10 s pause time was given between loading and unloading cycles.

A ball-on-disk tribometer (SENSE-7) was employed to measure the tribological properties of the coatings. The commercially obtained steel balls ($\varphi 6.25$ mm) were used as the counterpart. The friction tests were carried out at a reciprocating sliding velocity of 4 m/s under a load 6 N for a distance of 60 m, and the sliding stroke was around 1.00 mm. Each of these tests was repeated three times. All the experiments were accomplished in ambient condition of temperature 25±1 °C and 50%±2% relative humidity. No lubrication was used during wear tests. The volumetric wear rate (R_w) of specimens was calculated by $R_w = V/F \cdot S$, where V is the wear volume (mm³), F is the applied load (N), and S is the sliding distance (m). The wear volume was obtained by a non-contact surface mapping profiler (ADE Corporation, USA).

3. RESULTS AND DISCUSSION

The SEM morphologies of the as-deposited and heat treated Cr–C coatings are displayed in Fig. 1. The as-deposited sample presents a typical nodular structure with some microcracks (red arrows in Fig. 1(a)) on the coating. It is believed that the reduction of hydrogen ions during the electrodeposition process results in hydrogen evolution and crack formation. In the case of Cr–C deposit annealed at 200 °C, an increase in the number of cracks in the Cr–C coating (red arrows in Fig. 1(b)) can be observed. A network structure of cracks all over the Cr–C coatings annealed at 400 °C and 600 °C is formed and the cracks become much wider and broader compared to the one annealed at 200 °C (Fig. 1(c) and (d)), The hardness of Cr–C coatings will be significantly enhanced due to the precipitation of Cr_{23}C_7 , and Cr_7C_3 during heating [25,26]. In general, the enhanced hardness of metal materials also will decrease the toughness of metals (or enhance its brittleness), leading to the reduction in fracture toughness and yield stress [27].

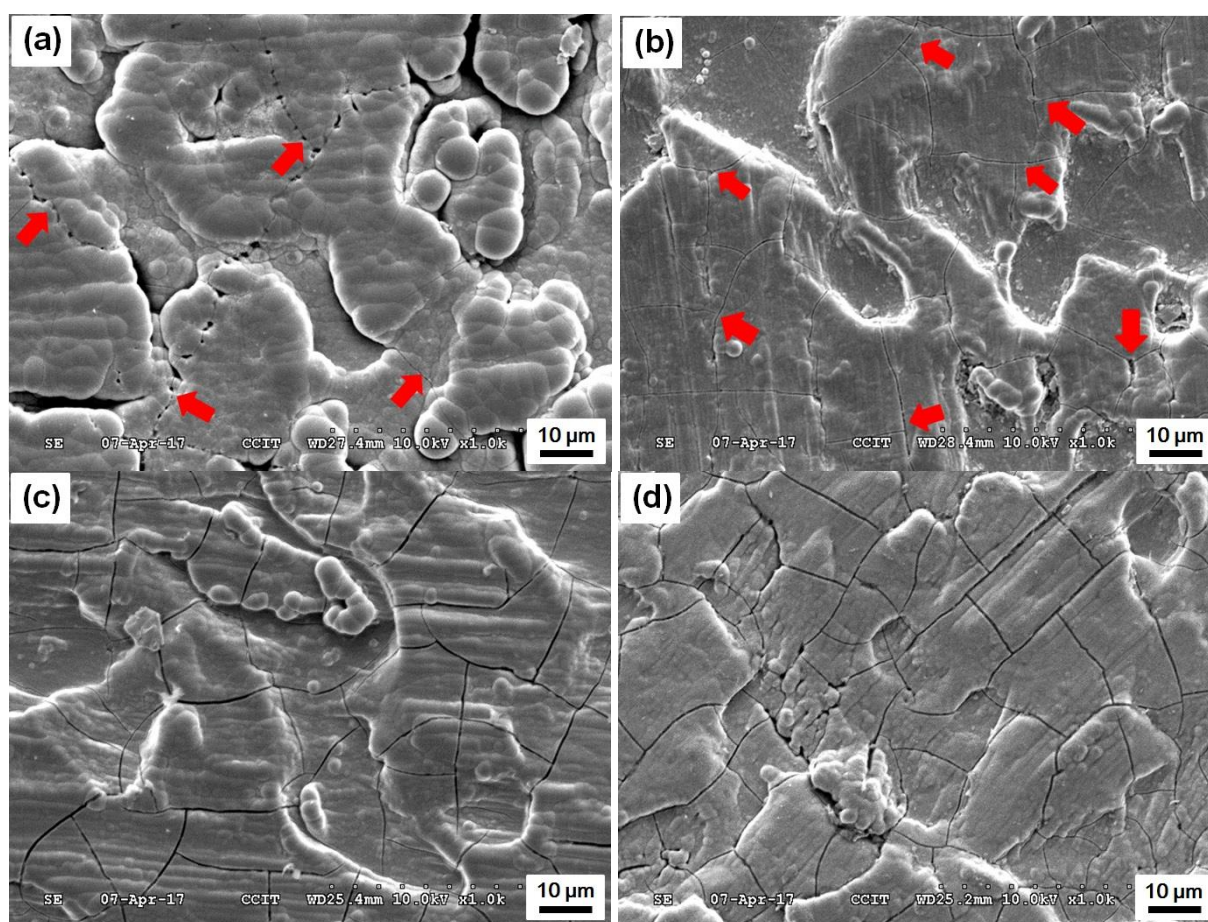


Figure 1. SEM surface morphologies of Cr–C coatings heated at various temperatures: (a) as-plated, (b) 200 °C, (c) 400 °C and (d) 600 °C.

Consequently, the materials with a high hardness will be fractured easily by various stresses such as thermal stress, residual stress and impact stress etc. Therefore, one possible explanation for the increase of microcrack density by annealing is due to the release of internal (residual) stress [28]. In addition, owing to the different thermal expansion coefficients between steel substrates (about $13 \times 10^{-6} \text{ } ^\circ\text{C}^{-1}$) and Cr coatings (about $6.2 \times 10^{-6} \text{ } ^\circ\text{C}^{-1}$), the thermal stress will be generated during the heat

treatment, resulting in the formation of the cracks. However, the change of phase structure from amorphous to crystalline might also has some influence on it.

Fig. 2 shows the morphologies of the as deposited and heat treated Cr-C/Al₂O₃ composite coatings. It shows from Fig. 2(a) that no cracks are seen on the as deposited Cr-C/Al₂O₃ composite coating. On annealing Cr-C/Al₂O₃ coating at 200 °C the crack free microstructure is maintained (Fig. 2(b)). At higher annealing temperatures of 400 °C and 600 °C (Fig. 2(c) and 2(d)), a network of cracks occurs and the density of cracks network within Cr-C/Al₂O₃ composite coatings becomes less dense as the heat treatment temperature increasing. The obvious network of cracks appears in Cr-C/Al₂O₃ composite coatings heated at higher temperature can be mainly attributed to the effect of thermal stress. It shows from Fig. 2(b) that the, this indicates the added Al₂O₃ particles can reduce the internal (residual) stress of coatings during electroplating process and this result is also in agreement with our previous study [25]. Fig. 3 presents SEM cross-sectional images for the as-plated coatings of Cr-C coatings and Cr-C/Al₂O₃ composite coating, respectively.

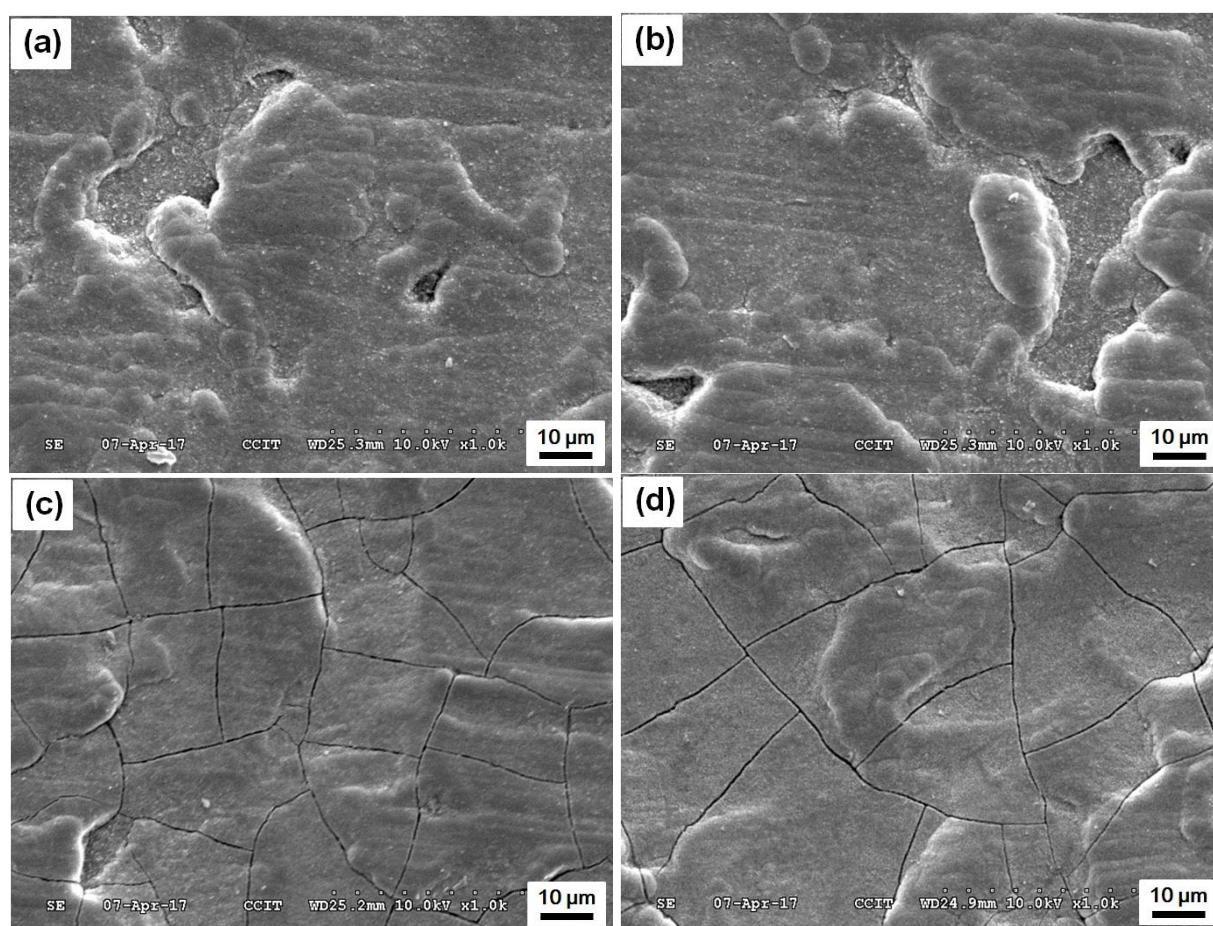


Figure 2. Surface morphologies Cr-C/Al₂O₃ composite deposit heated at various temperatures: (a) as-plated, (b) 200 °C, (c) 400 °C and (d) 600 °C.

Fig. 3(a) indicates that the cracks caused by internal (residual) stress during electroplating process penetrate through the Cr-C coating and reach the steel surface. Fig. 3(b) shows a crack-free

structure took place within Cr-C/Al₂O₃ composite coating due to incorporation of these dispersion Al₂O₃ particles into the Cr-C deposit leads to the reduction of the coating internal stresses [25].

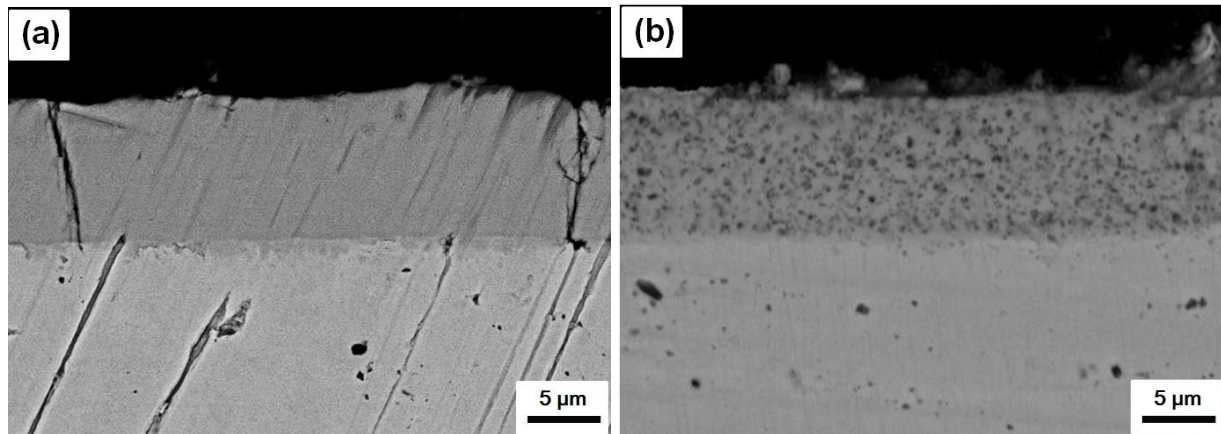


Figure 3. SEM cross-sectional images of the as-plated coatings: (a) Cr-C coating, (b) Cr-C/Al₂O₃ composite coating.

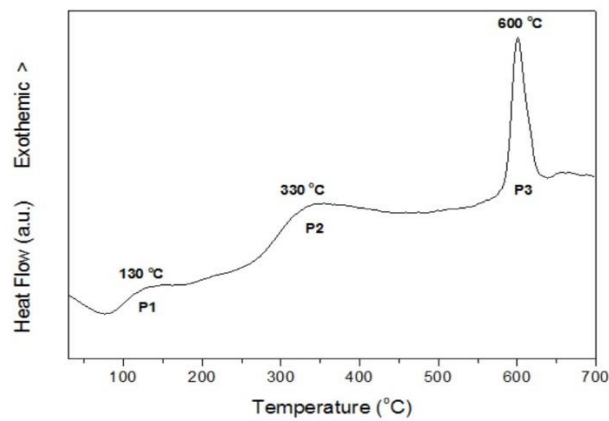
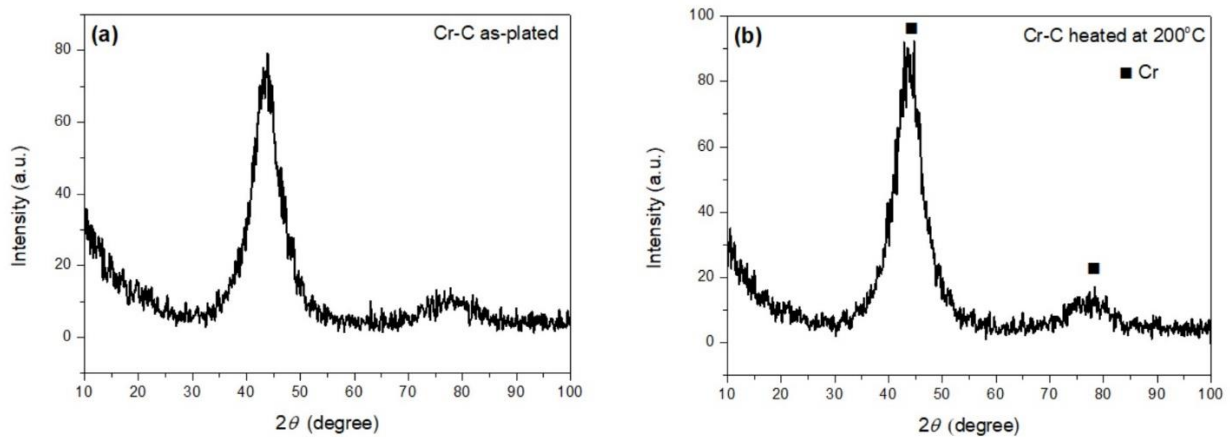


Figure 4. DSC curve of the as-plated Cr-C coating tested in a flowing nitrogen atmosphere and with a heating rate of 20 °Cmin⁻¹.



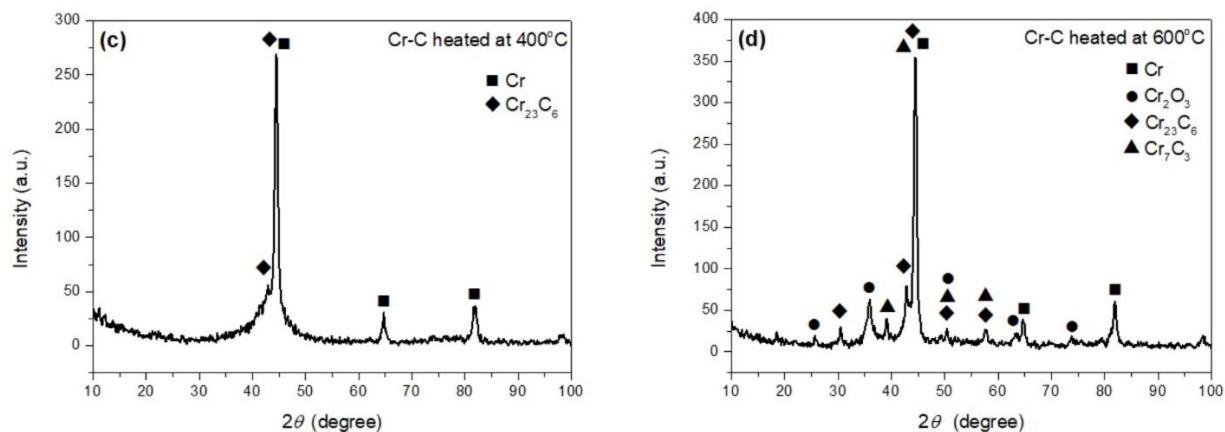


Figure 5. The X-ray diffraction patterns of Cr-C coatings after annealing at different temperatures: (a) as-plated, (b) annealed at 200 °C, (c) annealed at 400 °C, and (d) annealed at 600 °C.

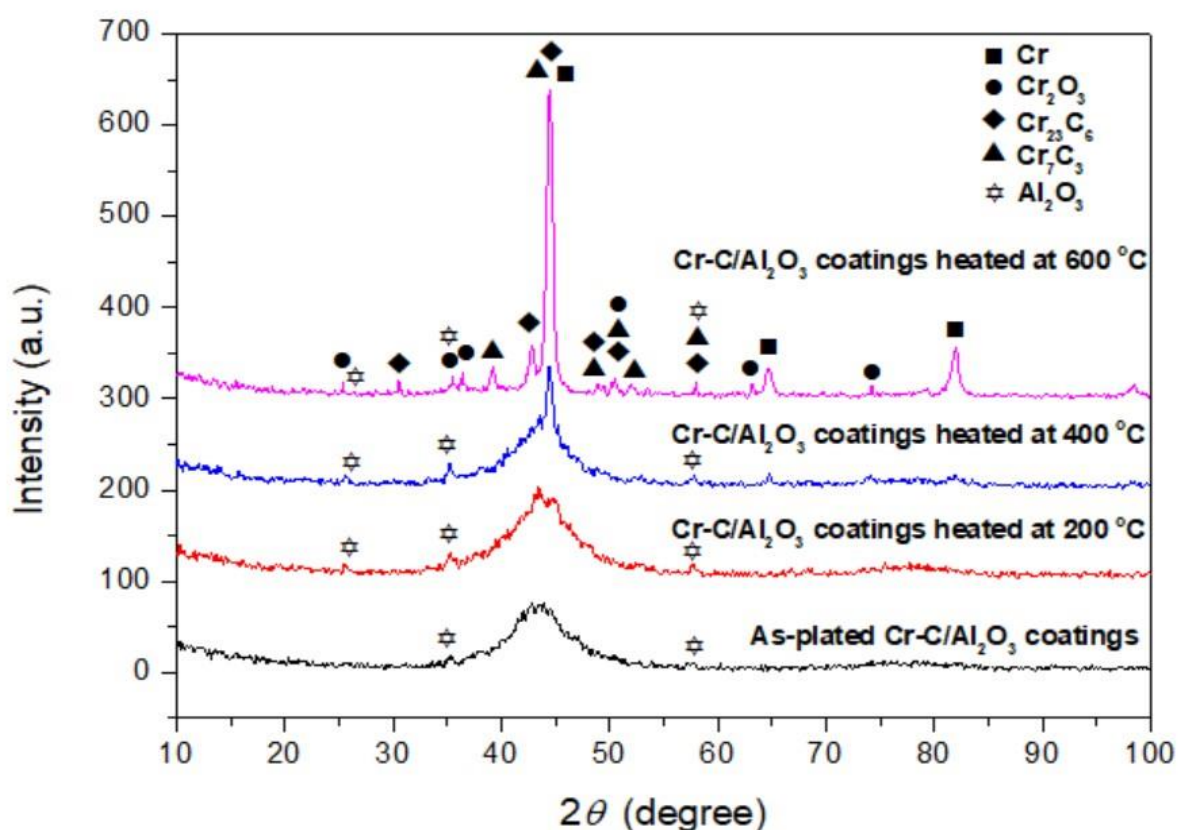


Figure 6. The X-ray diffraction patterns of Cr-C/Al₂O₃ composite coatings after annealing at different temperatures.

DSC result under a heating rate of 20 °C/min is shown in Fig. 4. Three exothermic peaks can be observed during heating up to 700 °C, which indicates that three phase transformations occur. The peak temperature corresponding to each phase transformation is approximately at 130, 330 and 600 °C, respectively. In order to identify the phase transformation of the three exothermic steps, the Cr-C coating was annealed at 200, 400 and 600 °C for 1 h, respectively. The phase evolution was analyzed by X-ray diffraction, and the XRD patterns of Cr-C coatings as a function of annealing temperature

are shown in Fig. 5. Fig. 5(a) shows that the as deposited Cr–C coating is amorphous. As shown in Fig. 5(b), a sharp peak exists together with the broad peak around at $2\theta = 43.5^\circ$ was observed for the Cr–C coating annealed at 200 °C, indicating the Cr–C coating starts to crystallize at temperatures lower than 200 °C. However, the crystallization is not completed until 400 °C. Fig. 5(c) presents that the appearance of Cr and Cr_{23}C_6 peaks after the Cr–C coatings heating at 400 °C. When the Cr–C coatings are heated at 600 °C, the diffraction peaks indicated Cr, Cr_{23}C_6 , Cr_7C_3 and Cr_2O_3 appear in the XRD pattern (Fig. 5(d)). The above results are in agreement with previous studies that the Cr–C coatings heated at 600 °C will precipitate Cr_{23}C_6 and Cr_7C_3 phases and enhance the hardness of coatings [25,26,29].

By comparing Fig. 4 and Fig.5, we can conclude that the exothermic peak “P1” in the range from 100 to 180 °C is related to the partial crystallization of chromium within Cr–C coating, peak “P2” in the range from 280 to 400 °C can be attributed to the formation of Cr_{23}C_6 phase and re-crystallization of Cr, peak “P3” in the range from 560 to 620 °C should be the formation of Cr_7C_3 and Cr_2O_3 . The Cr–C/ Al_2O_3 composite coatings present a similar XRD pattern with that of Cr–C coating, both in as plated and heat-treated conditions (Fig. 6). The X-ray diffraction angles occurred at 25.5° , 35.3° and 58° indicate the existence of Al_2O_3 particles within Cr–C matrix.

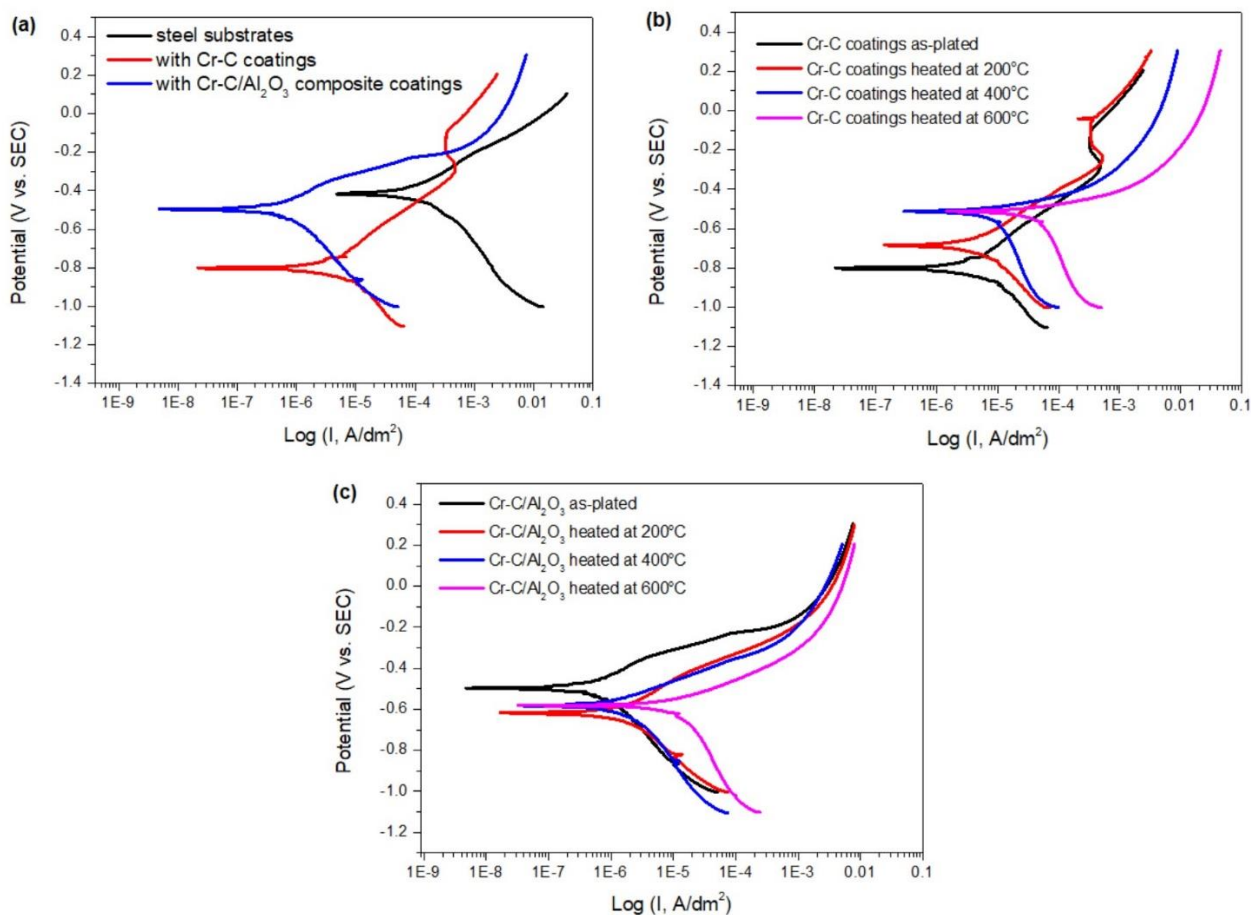
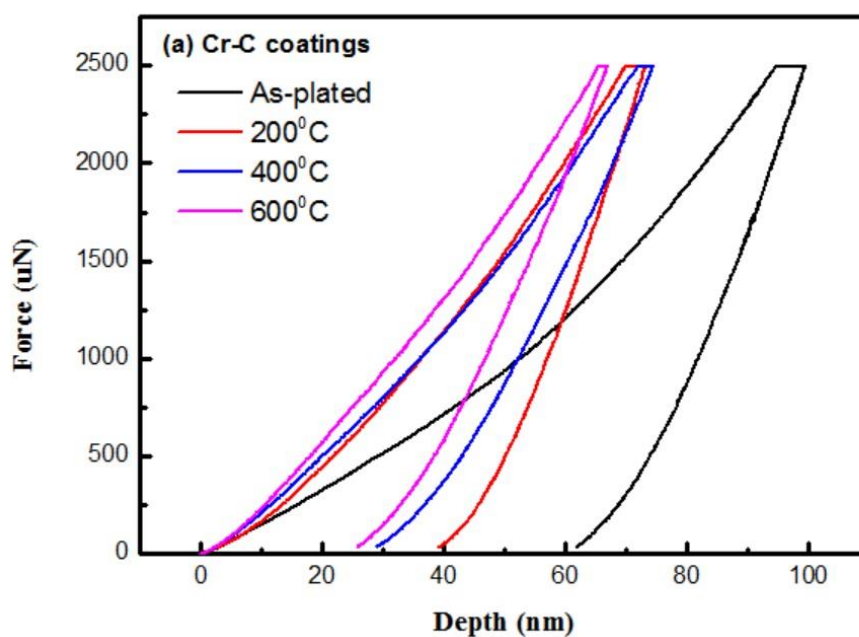


Figure 7. Potentiodynamic polarization curves of Cr–C coatings and Cr–C/ Al_2O_3 composite coatings: (a) as-plated Cr–C coatings and Cr–C/ Al_2O_3 composite coatings, (b) Cr–C coatings with heat treatment, (c) Cr–C/ Al_2O_3 composite coatings with heat treatment.

Fig. 7 shows the potentiodynamic polarization curves of the as-plated Cr-C coatings, as-plated Cr-C/Al₂O₃ composite coating and the coatings heated at various temperature. The corrosion potentials (E_{corr}), corrosion current densities (i_{corr}), anodic and cathodic Tafel slopes (β_a and β_c) derived from the potentiodynamic polarization curves of steel substrates, as-plated coatings and coatings after heating at different temperature were also presented in Table 1.

Table 1. Corrosion characteristics of Cr-C coatings and Cr-C/Al₂O₃ composite coatings heated at various temperature measured from 3.5 wt.% NaCl solution.

Sample code	β_a (V/ decade)	β_c (V/ decade)	i_{corr} (A/dm ²)	E_{corr} (V vs. SEC)
Steel substrates	0.215	-0.305	4.83×10^{-5}	-0.41
As-plated Cr-C coatings	0.267	-0.364	1.31×10^{-6}	-0.80
Cr-C coatings heated at 200°C	0.254	-0.355	2.34×10^{-6}	-0.69
Cr-C coatings heated at 400°C	0.238	-0.378	6.56×10^{-6}	-0.52
Cr-C coatings heated at 600°C	0.226	-0.381	2.19×10^{-5}	-0.52
As-plated Cr-C/Al ₂ O ₃ composite coatings	0.283	-0.375	2.84×10^{-7}	-0.50
Cr-C/Al ₂ O ₃ composite coatings heated at 200°C	0.256	-0.368	5.42×10^{-7}	-0.62
Cr-C/Al ₂ O ₃ composite coatings heated at 400°C	0.238	-0.346	8.62×10^{-7}	-0.58
Cr-C/Al ₂ O ₃ composite coatings heated at 600°C	0.223	-0.356	4.11×10^{-6}	-0.58



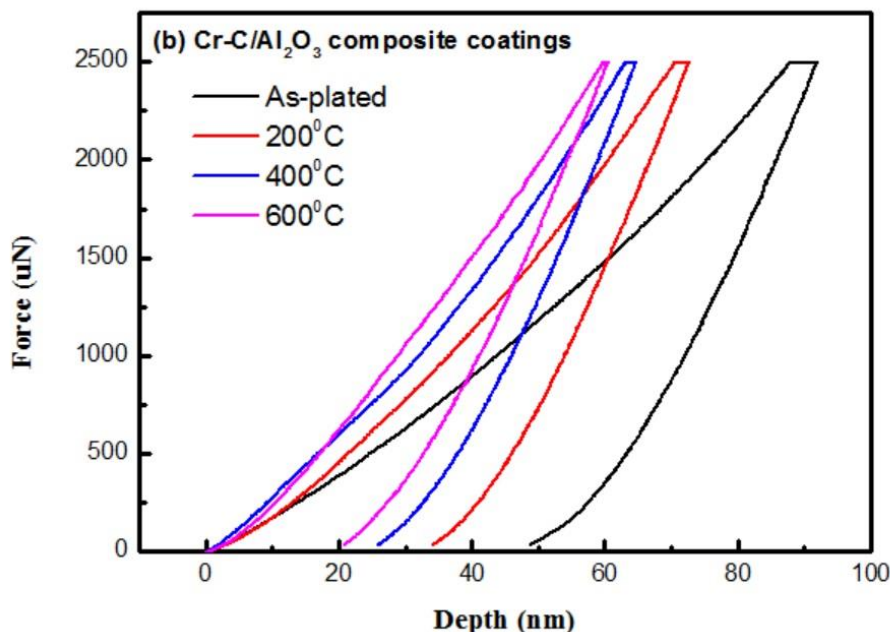


Figure 8. Loading-unloading curves of various coatings after annealing at different temperatures: (a) Cr-C coatings, (b) Cr-C/Al₂O₃ composite coatings.

Fig. 7(a) presents both Cr-C coatings and Cr-C/Al₂O₃ composite coatings has excellent corrosion resistance than that of steel substrates, and their i_{corr} is approximately at 1.31×10^{-6} and 2.84×10^{-7} A/dm², respectively. It also can see that the corrosion resistance of Cr-C/Al₂O₃ composite coatings is better than that of Cr-C coatings, it can be attributed to the Cr-C/Al₂O₃ composite coatings has a cracks-free structure (see Fig. 1(a) and Fig. 2(a)) that can obstruct the corrosion factors to corrode the substrates along the cracks within coatings. In Table 1, the i_{corr} of Cr-C coatings decrease with the increasing of heat temperature from 1.31×10^{-6} A/dm² to 2.19×10^{-5} A/dm². The same condition also occurred at Cr-C/Al₂O₃ composite coatings, but the Cr-C/Al₂O₃ composite coatings still maintain an excellent anti-corrosion behavior (2.84×10^{-7} to 8.62×10^{-7} A/dm²) until heated at 400°C, the i_{corr} also still keep at 4.11×10^{-6} A/dm² after heating at 600°C. The corrosion resistance of Cr-C/Al₂O₃ composite coatings are significantly better than that of Cr-C coatings after heat treatment, due to the added Al₂O₃ particles will reduce the internal stress of Cr-C matrix [25] and inhibit the formation of cracks within Cr-C matrix during heating process.

Nano-indentation test can reflect the hardness of materials [30] and the elastic modulus of the thin films is an important mechanical property of the coatings [31]. Besides, hardness and elastic modulus can be affected by various factors such as microstructure and heat treatment [32]. To evaluate the mechanical properties of Cr-C coatings and Cr-C/Al₂O₃ composite coatings after heat treatment, the micro-hardness of various coatings are performed by nano-indentation tests. The typical displacement-load curves of the Cr-C coatings and Cr-C/Al₂O₃ composite coatings are shown in Fig. 8. The average hardness values of five independent measurement points in each sample measured by nano-indentation are shown in Fig. 9.

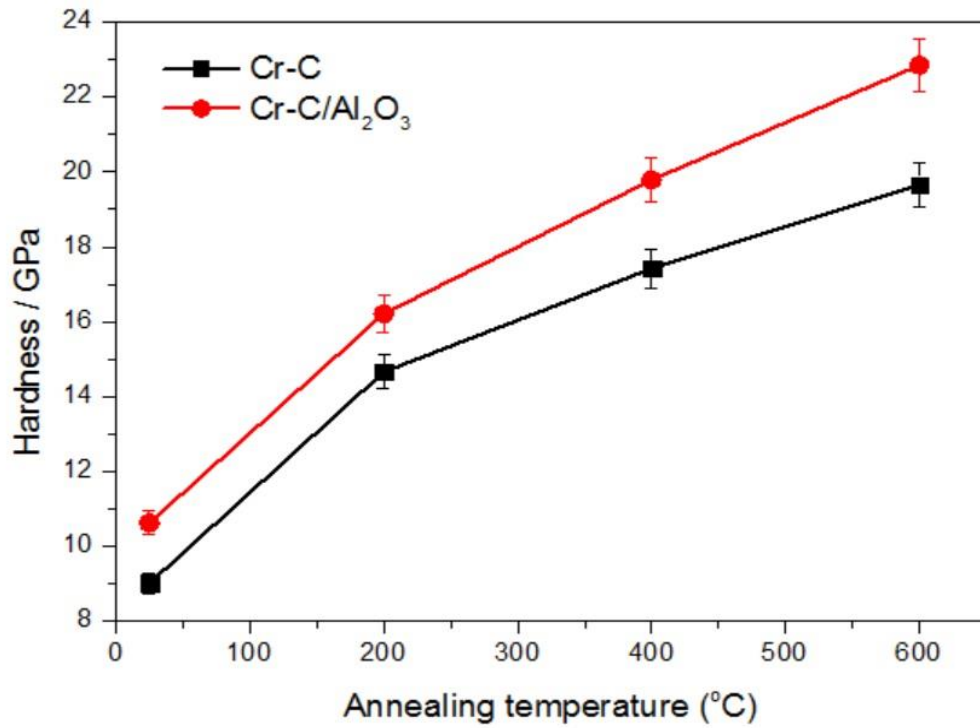
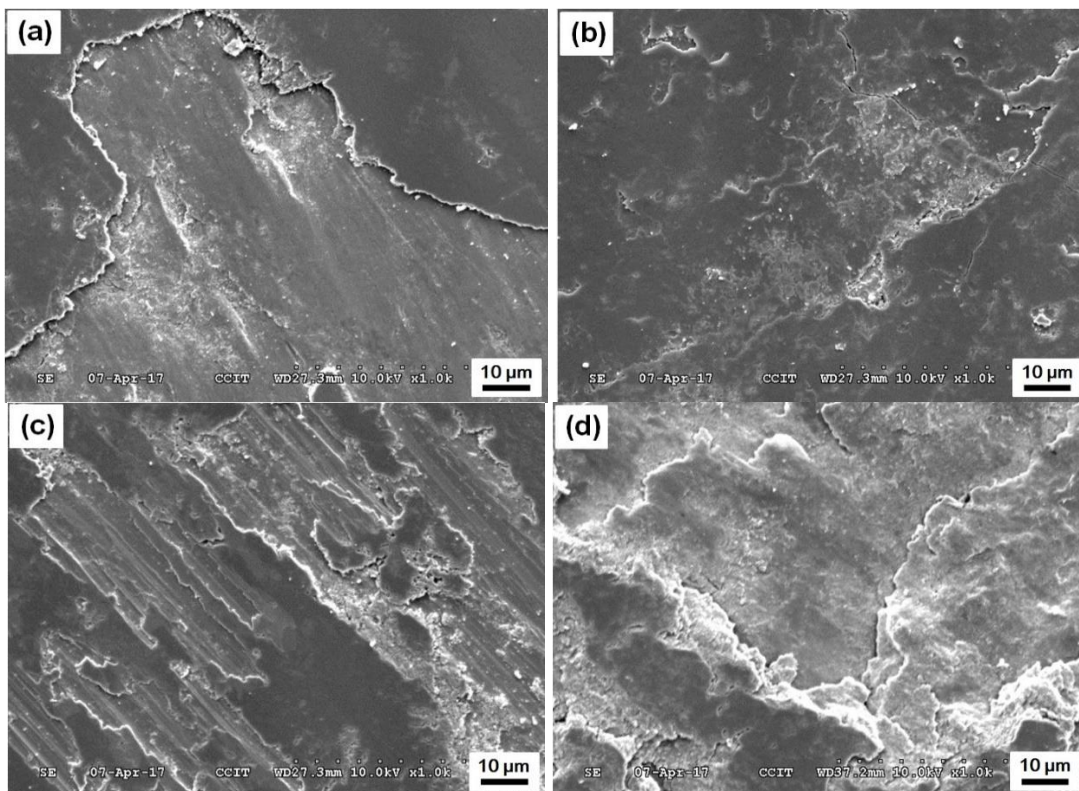


Figure 9. Effect of annealing temperature on the hardness of Cr–C coating and Cr–C/Al₂O₃ composite coating.



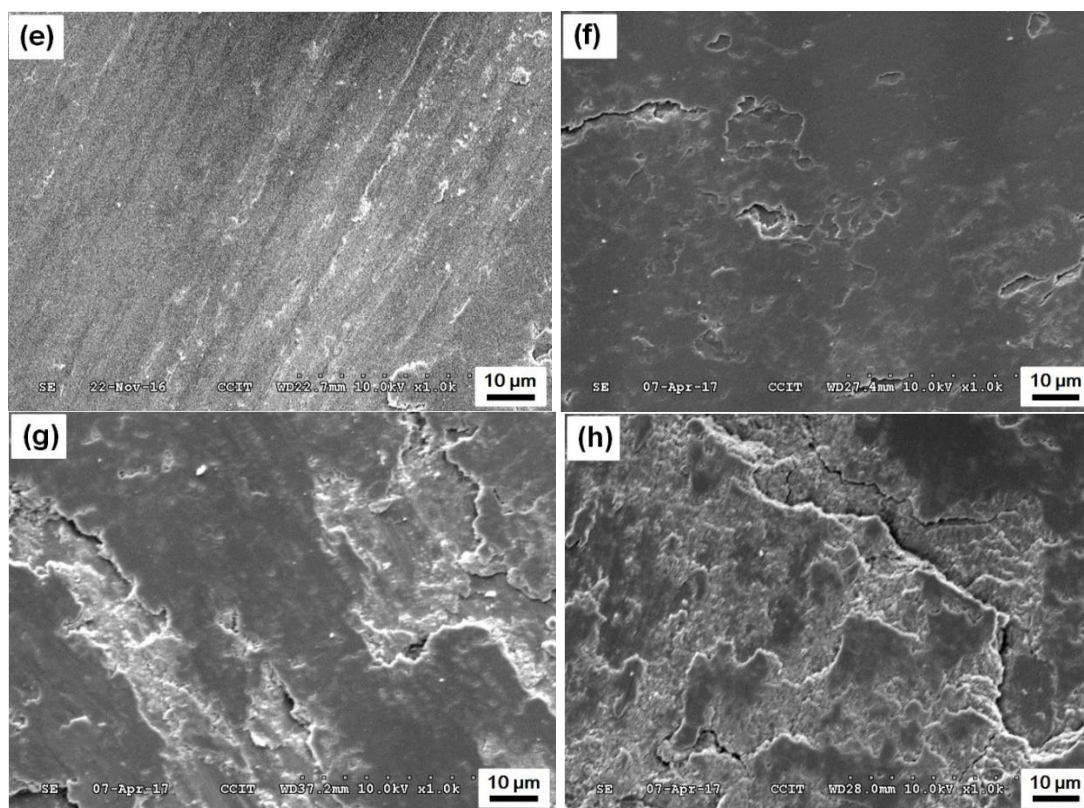


Figure 10. SEM morphologies of the worn surfaces of Cr–C coatings (a) as-deposited, (b) annealed at 200 °C, (c) annealed at 400 °C, (d) annealed at 600 °C and Cr–C/Al₂O₃ composite coatings (e) as-deposited, (f) annealed at 200 °C, (g) annealed at 400 °C, (h) annealed at 600 °C.

The dynamic micro-hardness of Cr–C coatings and Cr–C/Al₂O₃ composite coatings analyzed by a nano-indentation test can be calculated using the formula developed by Oliver et al. [33] as follows:

$$H = \frac{P_{max}}{A_c} = \frac{(\alpha \times P_{max})}{h_c^2} \quad (1) \text{ where } H, P_{max}, h_c \text{ and } A_c \text{ defined as the dynamic}$$

micro-hardness, the peak load, the contact depth, and contact area, respectively. α was a constant that depends on the indenter shape. In this study, α was kept at 15.08, which corresponded to the indenter with a tip angle of 100°.

Fig. 9 presents the hardness of Cr–C coatings and Cr–C/Al₂O₃ composite coatings annealed at various temperatures. The hardness of samples increases with increasing of heat treatment temperature and the hardness of Cr–C/Al₂O₃ composite coatings is higher than that of Cr–C coatings when annealing at same temperature. The Cr–C and Cr–C/Al₂O₃ composite coating exhibit the maximum hardness of 19.42 and 22.85 GPa, respectively, at the annealing temperature of 600 °C. The likely explanation to the enhancement of microhardness of these Cr–C and Cr–C/Al₂O₃ composite coating is the crystallization of Cr and the precipitation of Cr₂₃C₆, Cr₇C₃ and Cr₂O₃ phases occurs at 600 °C, which can be found clearly in the XRD patterns (see Fig. 5 and 6). Based on the XRD data shown in Fig. 5 and Fig. 6, Scherrer's equation was utilized to calculate grain size. The grain size of Cr–C coating and Cr–C/Al₂O₃ composite coating annealed at different temperatures is listed in Table 2.

Table 2. The grain size of Cr–C coatings and Cr–C/Al₂O₃ composite coatings annealed at different temperatures

Samples	Crystallite size (nm)			
	As-plated	H.T. 200 °C	H.T. 400 °C	H.T. 600 °C
Cr–C	amorphous-like	3.1	17.9	29.6
Cr–C/Al ₂ O ₃	amorphous-like	1.5	4.8	18.5

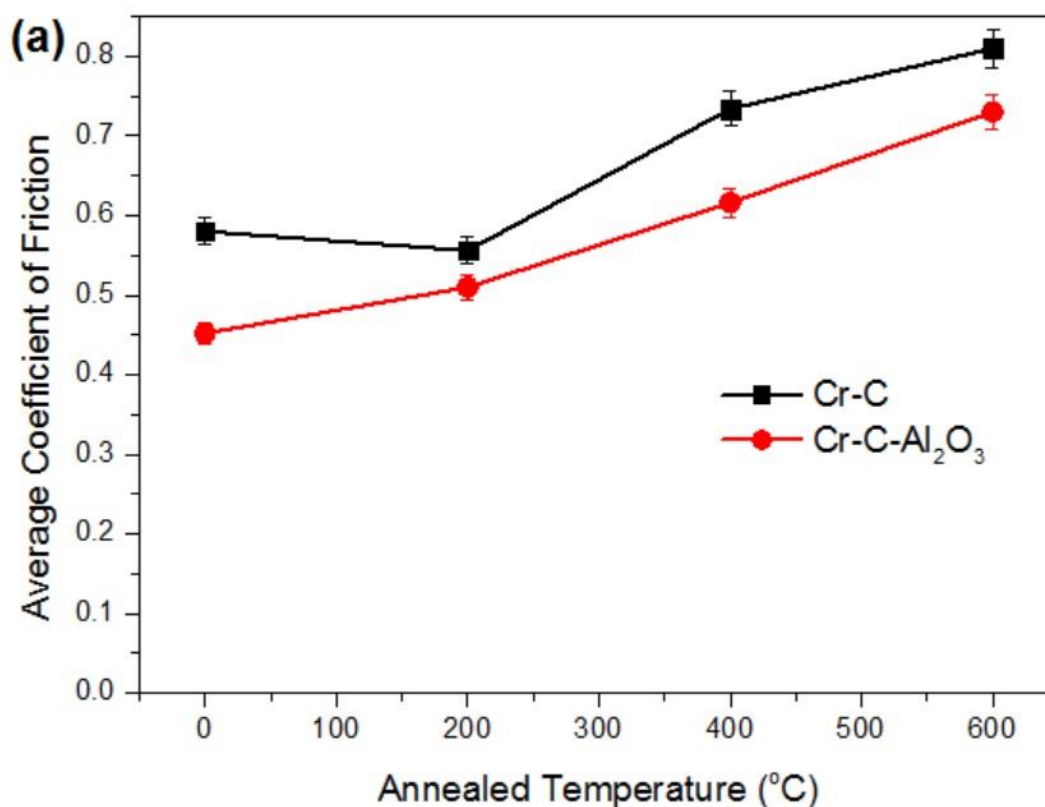
It was found that the grain size increased with increased annealing temperature. The grain size for the Cr–C coating annealed at 200 °C was 3.1 nm and increased to 17.9 nm at 400 °C and to 29.6 nm at 600 °C. In the case of Cr–C/Al₂O₃ composite coating the grain size for the coating annealed at 200 °C was 1.5 nm and increased to 4.8 nm at 400 °C and to 18.5 nm at 600 °C. The grain size of Cr–C/Al₂O₃ composite coatings is smaller than that of the relevant Cr–C coatings, this can be attributed to the incorporation of Al₂O₃ particles in the coating will hinder the grain growth during heat treatment [34,35]. According to the Halle-Petch equation [36] the micro-hardness varies linearly with the inverse square root of the grain diameter. This relationship indicates that the hardness increases with decreasing grain size. As mentioned above, the hardness of Cr–C/Al₂O₃ composite coating is higher than that of relevant Cr–C coating, both in as plated and heat-treated conditions. The mechanisms of such strengthening are the grain refinement strengthening and the dispersion strengthening effect caused by the Al₂O₃ particles uniformly distributed in the Cr–C matrix.

The worn surface morphologies for as-plated and heat treated Cr–C coatings and Cr–C/Al₂O₃ composite coatings are presented in Fig. 10. The as-plated Cr–C coating shows typical adhesive wear morphology with large debris formed on the worn surface (Fig. 10(a)). The formation of large debris and severe adhesive wear are indicative of poor wear resistance of as-plated Cr–C coating. Fig. 10(b) presents the micrographs of worn surface of Cr–C coating after heat treated at 200 °C. After heating at 200 °C, Fig. 10(b) exhibits some characteristics of adhesive wear and no debris appears on the surface. As it was mentioned before, the as-deposited Cr–C coating has a hardness of 9.3 GPa and the hardness increases to 14.22 GPa as the samples annealed at 200 °C. Therefore, the reduction in the adhesive wear might be attributed to the increase of hardness of the coating due to the heat treatment at 200 °C. After annealing at 400 and 600 °C, the mechanism moves towards abrasive wear characterized by extensive plastic deformation, deep grooves and severe disruption on worn surface as shown in Fig. 10(c) and 10(d). After heat treatment at 400 and 600 °C, the Cr–C coatings become much harder and more brittle due to the precipitation of Cr₂₃C₆, Cr₇C₃ and Cr₂O₃. During the wear test, a part of the coating will be peeled off as chips and stuck between the counter ball and the surface of Cr–C coatings, the surface of coatings will be seriously scratched by chips and caused a micro-cutting action during sliding process. This kind of micro-cutting action caused by detached Cr–C debris can act as the hard third body abrasives [37]. Fig. 10(e) represents the wear tracks of the as-plated Cr–C/Al₂O₃

composite coatings. The adhesive wear appears to be the most likely wear behavior for as-plated Cr–C/Al₂O₃ composite coating, as supported by only slight abrasive grooves caused by the plowing process appears on the worn surface. Fig. 10(f) shows the worn surface of Cr–C/Al₂O₃ composite coatings after heating at 200 °C. The abrasive grooves caused by the plowing process are not found due to the hardness of composite coating increase to 16.18 GPa. Fig. 10(g) and (h) show the worn surface of Cr–C/Al₂O₃ composite coatings annealed at 400 and 600 °C, respectively. The wear caused by the effect of hard third body abrasives is evident on the worn surface of Cr–C/Al₂O₃ composite coatings which is similar to that of the relevant Cr–C coatings (Fig. 10(c) and (d)). This might contribute to a significant increase in specific wear rate of coatings.

Fig. 11 shows the annealing temperature effect on friction coefficients and wear rate of the Cr–C coatings and Cr–C/Al₂O₃ composite coatings. It can be clearly seen from Fig. 11(a) that the average friction coefficients of Cr–C/Al₂O₃ composite coatings (from 0.45 to 0.73) are lower than that of the relevant Cr–C coatings (from 0.55 to 0.81). This can be attributed to the improvement of hardness of Cr–C coatings caused by the combine effect of grain size refining and Al₂O₃ particles dispersion strengthening (Fig. 9). It leads to a decrease in the average friction coefficients between the counter ball and coatings due to the inert particles uniformly distributed in the metal matrix could restrain the growth of the alloy grains and the plastic deformation of the matrix under a loading [38].

Fig. 11(b) shows the annealing temperature effect on wear rate of the Cr–C coatings and Cr–C/Al₂O₃ composite coatings, both in as plated and heat-treated conditions. The specific wear rate of as-plated Cr–C coatings and as-plated Cr–C/Al₂O₃ composite coatings is approximately at $47.49 \times 10^{-7} \text{ mm}^3/\text{Nm}$ and $15.53 \times 10^{-7} \text{ mm}^3/\text{Nm}$, respectively.



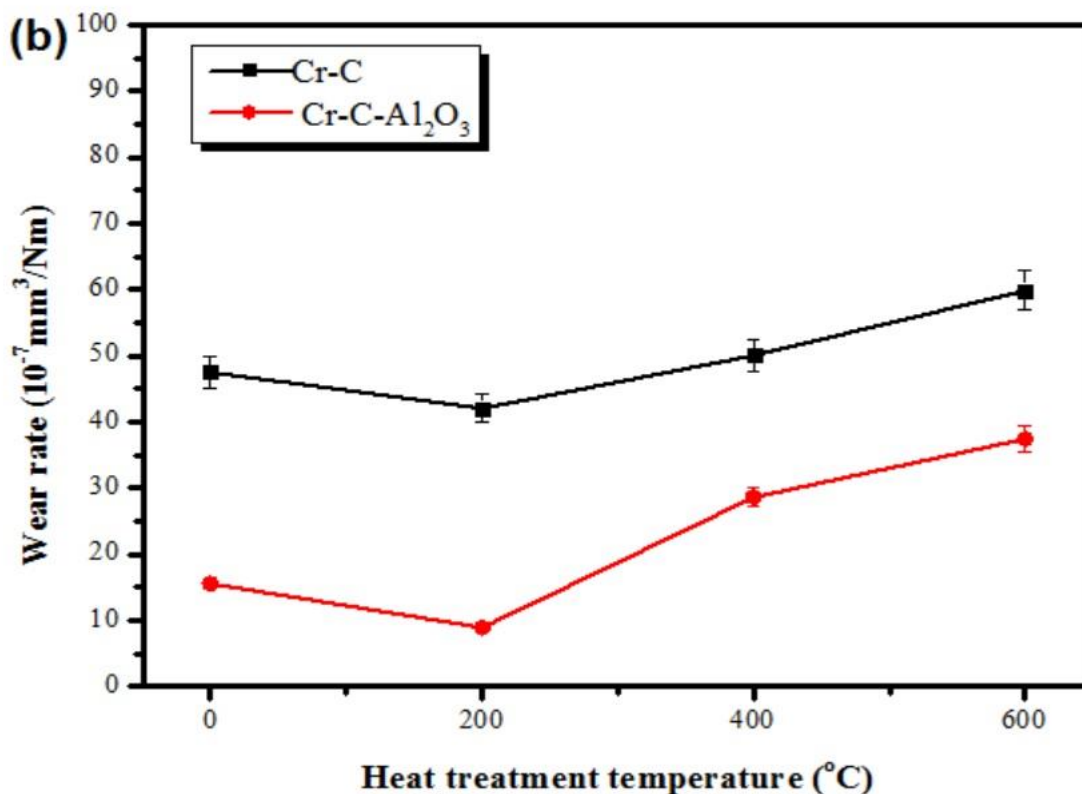


Figure 11. The effect of annealing temperature on: (a) average of friction coefficient and (b) wear rate of Cr–C coating and Cr–C/Al₂O₃ composite coating.

The result of wear rate indicates the incorporation of Al₂O₃ particles into the Cr–C matrix will significantly enhance the wear resistance of coatings due to the Al₂O₃ dispersion strengthening effect enhances the hardness of the as-deposited coating from 9.02 to 10.63 GPa (Fig. 9). The lowest specific wear rate ($8.8 \times 10^{-7} \text{ mm}^3/\text{Nm}$) was achieved for Cr–C/Al₂O₃ composite coating annealed at 200°C. The increase of annealing temperature leads to a lower specific wear resistance. When the annealing temperature increases from 400 to 600 °C, the specific wear rate of Cr–C coating and Cr–C/Al₂O₃ composite coating significantly increase from 42.02 to $59.84 \times 10^{-7} \text{ mm}^3/\text{Nm}$ and 8.8 to $37.4 \times 10^{-7} \text{ mm}^3/\text{Nm}$, respectively. The increased specific wear rate of coatings can be attributed to the higher hardness (over 17.42 GPa) of coatings results in the occurrence of hard third body abrasives during wear resistance test.

4. CONCLUSIONS

In the present study, the effect of heat treatment on the corrosion resistance, mechanical properties and tribological behavior between Cr–C coatings and Cr–C/Al₂O₃ composite coatings were examined and compared, the following conclusions have been drawn:

(1) The incorporation of Al₂O₃ particles into the Cr–C matrix can reduce the internal stress. No crack was found on the surface of as-deposited Cr–C/Al₂O₃ composite coating and the crack-free

structure was maintained for the coating after annealing at 200 °C.

(2) The Cr–C/Al₂O₃ composite coatings has the best corrosion resistance ($i_{\text{corr}} = 2.84 \times 10^{-7}$ A/dm²) due to a crack-free structure within Cr–C matrix.

(3) The hardness of Cr–C/Al₂O₃ composite coatings is higher than that of Cr–C coatings, both in as plated and heat-treated conditions. The improvement of hardness can be attributed to the combine effect of grain size refining and Al₂O₃ particles dispersion strengthening. The highest microhardness of Cr–C/Al₂O₃ composite coating (22.85 GPa) was achieved for Cr–C/Al₂O₃ composite coating after annealing at 600 °C.

(4) The codeposition of Al₂O₃ particles within the Cr–C deposits will significantly improve the wear resistance of coatings and reduces the wear weight loss. The lowest specific wear rate (8.8×10^{-7} mm³/Nm) was obtained for the Cr–C/Al₂O₃ composite coatings heat treated at 200 °C.

References

1. S. Ghaziof, M.A. Golozar, K. Raeissi, *J. Alloys Compd.*, 496 (2010) 164.
2. Z. Zeng, L. Wang, A. Liang, J. Zhang, *Electrochim. Acta*, 52 (2006) 1366.
3. F.I. Danilov, V.S. Protsenko, V.O. Gordiienko, S.C. Kwon, J.Y. Lee, Kim M., *Appl. Surf. Sci.*, 257 (2011) 8048.
4. H. Yu, B. Chen, H. Wu, X. Sun, B. Li, *Electrochim. Acta*, 54 (2008) 720.
5. H.H. Sheu, C.H. Lin, S.Y. Jian, H.B. Lee, B.R. Yang, M.D. Ger, *Int. J. Electrochem. Sci.*, 11 (2016) 7099.
6. S.C. Kwon, M. Kim, *Surf. Coat. Technol.*, 158 (2004) 151.
7. G. Saravanan, S. Mohan, *Corros. Sci.*, 51 (2009) 197.
8. Y.B. Song, D.T. Chin, *Electrochim. Acta*, 48 (2002) 349.
9. C.W. Chien, C.L. Liu, F.J. Chen, K.H. Lin, C.S. Lin, *Electrochim. Acta*, 72 (2012) 74.
10. S. Surviliene, A. Lisowska-Oleksiak, V. Jasulaitiene, A.C. Esuniene, *Trans IMF*, 83 (2005) 130.
11. Q. Feng, T. Li, H. Yue, K. Qi, F. Bai, J. Jin, *Appl. Surf. Sci.*, 254 (2008) 2262.
12. Z. Zeng, J. Zhang, *Surf. Coat. Technol.*, 202 (2008) 2725.
13. J.N. Balaraju, V. Ezhil Selvi, K.S. Rajam, *Mater. Chem. Phys.*, 120 (2010) 546.
14. S. Surviliene, V. Jasulaitiene, A. Lisowska-Oleksiak, V.A. Safonov, *J. Appl. Electrochem.*, 35 (2005) 9.
15. M.H. Sarafrazi, M. Alizadeh, *J. Alloys Compd.*, 720 (2017) 289.
16. H.T. Wang, H.H. Sheu, M.D. Ger, K.H. Hou, *Surf. Coat. Technol.*, 259 (2014) 268.
17. P.L. Mangonon, *Principles of materials selection for engineering design*. Prentice Hall, London (1998).
18. Z. Zeng, J. Zhang, *Surf. Coat. Technol.*, 202 (2008) 2725.
19. M. Salehi Doolabi, S.K. Sadrnezhaad, D. Salehi Doolabi, M. Asadirad, *International Heat Treatment and Surface Engineering*, 6 (2012) 178.
20. M. Salehi Doolabi, S.K. Sadrnezhaad, D. Salehi Doolabi, *Anti-Corrosion Methods and Materials*, 61 (2014) 205.
21. K.H. Hou, M.C. Jeng, M.D. Ger, *J. Alloys Compd.*, 437 (2007) 289.
22. A. Martín, J. Rodríguez, J. Llorca, *Wear*, 225–229 (1999) 615.
23. I. Apachitei, F.D. Tichelaar, J. Duszczuk, L. Katgerman, *Surf. Coat. Technol.*, 149 (2002) 263.
24. A. Liang, L. Ni, Q. Liu, J. Zhang, *Surf. Coat. Technol.*, 218 (2013) 23.
25. H.H. Sheu, C.E. Lu, K.H. Hou, M.L. Kuo, M.D. Ger, *Journal of the Taiwan Institute of Chemical Engineers*, 48 (2015) 73.
26. C.A. Huang, C.K. Lin, C.Y. Chen, *Surf. Coat. Technol.*, 203 (2009) 3686.

27. R. Furushima, K. Katou, S. Nakao, Z.M. Sun, K. Shimojima, H. Hosokawa, *International Journal of Refractory Metals and Hard Materials*, 42 (2014) 42.
28. C.A. Huang, W. Lin, S.C. Chen, M.C. Liao, *Mater. Sci. Eng. A*, 403 (2005) 222.
29. C.A. Huang, U.W. Lieu, C.H. Chuang, *Surf. Coat. Technol.*, 203 (2009) 2921.
30. H.F. Xuan, Q.Y. Wang, S.L. Bai, Z.D. Liu, H.G. Sun, P.C. Yan, *Surf. Coat. Technol.*, 244 (2014) 203.
31. M. Masanta, S.M. Shariff, *Mater. Sci. Eng. A*, 528 (2011) 5327.
32. G.F. Sun, R. Zhou, Y.K. Zhang, G.D. Yuan, K. Wang, X.D. Ren, D.P. Wen, *Optics Laser Technol.*, 62 (2014) 20.
33. W.C. Oliver, G.M. Pharr, *J. Mater. Res.*, 19 (2004) 3.
34. E. Budevski, G. Staikov, W.J. Lorenz, *Electrochim. Acta*, 45 (2000) 2559.
35. S.C. Wang, W.J. Wei, *J. Mater. Res.*, 18 (2003) 1566.
36. N.J. Petch, *Prog. Mater. Phys.*, 5 (1954) 1.
37. S. Mahdavi, S.R. Allahkaram, *J. Alloys Compd.*, 635 (2015) 150.
38. Y. Yao, S. Yao, L. Zhang, H. Wang, *Mater. Lett.*, 61 (2007) 67.

© 2018 The Authors. Published by ESG (www.electrochemsci.org). This article is an open access article distributed under the terms and conditions of the Creative Commons Attribution license (<http://creativecommons.org/licenses/by/4.0/>).